Hindawi
Journal of Nanomaterials
Volume 2019, Article ID 8932312, 10 pages
https://doi.org/10.1155/2019/8932312

Research Article

Study on the Relationship between Electrical Tree Development and Partial Discharge of XLPE Cables

Chaofei Gao,[1] **Yanlong Yu**,[2] **Zan Wang**,[1,3] **Wei Wang**,[1] **Liwei Zheng**,[1] **and Jian Du**[1]

[1]*State Key Laboratory of Alternate Electrical Power System with Renewable Energy Sources, North China Electric Power University, Beijing 102206, China*
[2]*Hangzhou Power Supply Bureaus, Hangzhou 310052, China*
[3]*State Grid Economic and Technological Research Institute Co. Ltd., Beijing 102209, China*

Correspondence should be addressed to Chaofei Gao; gao200401050208@126.com

Received 16 October 2018; Revised 10 January 2019; Accepted 20 February 2019; Published 1 April 2019

Guest Editor: Zhengping Zhou

Based on the slice materials of 35 kV and 110 kV XLPE cables, an experimental platform is built to study the relationship between electrical tree and PDs in XLPE with different voltage levels. There are three significant statistical characteristics of the PDs during the growth of electrical trees. The analysis of the results shows that each growth stage has certain characteristics. Different features existed between the growth of the electrical trees and the PD in the insulation of the 35 and 110 kV cables. Evident characteristics such as large spans of time and frequency were present as the electrical trees grew violently in the equivalent time-frequency diagram at every stage. These results could provide criteria for the identification of the deterioration using PD to monitor cables in service at rated voltages. The results are important for the identification of defects in cable insulation in order to provide an early warning of insulation breakdown in the cables.

1. Introduction

The study on the electrical trees and partial discharge of cross-linked polyethylene (XLPE) cables has been a critical issue for achieving better properties of XLPE cables [1–3]. Further, predictive maintenance of power cables plays an important role in effectively detecting and discovering insulation defects so that power grid interruptions caused by sudden power cable failure can be avoided [4, 5].

Partial discharge (PD) detection is recognized as the most direct and effective method to evaluate the insulation conditions of the cables [6–8]. However, no research has been down on how to estimate and forecast the degree of insulation defects based on the PD. It is important to forecast the insulation conditions of cables in order to find a standard to evaluate the severity of cable insulation defects through partial discharge detection [9].

Most insulation faults occur in cable accessories [10, 11]. Partial discharge is more likely to occur in the cable accessories due to their complex structure, concentrated electric field stress, and on-site construction. The breakdown of insulation in cable accessories is caused by lateral slip flash discharges between the stress cone and XLPE insulation [12, 13], as well as longitudinal dendritic discharge in XLPE insulation, which is the major form of discharge. These discharges initially develop from small PD [14–16]. Consequently, it necessitates more complete understanding of the relationship between electrical tree development and partial discharge of XLPE cables [17, 18]. It is of great importance for the online diagnosis of cable defects in PD detection to provide an early warning [19].

In this paper, the characteristics of PD during the electrical tree growth process in the insulations of 35 kV and 110 kV XLPE cables were studied by monitoring partial discharge and observing the growth of electrical trees using a digital microscope. The results can provide criteria for the identification of defects in the cable insulation in online monitoring of PD.

Although widely used in the study of electrical trees, the majority of microscopes are used to study the morphological

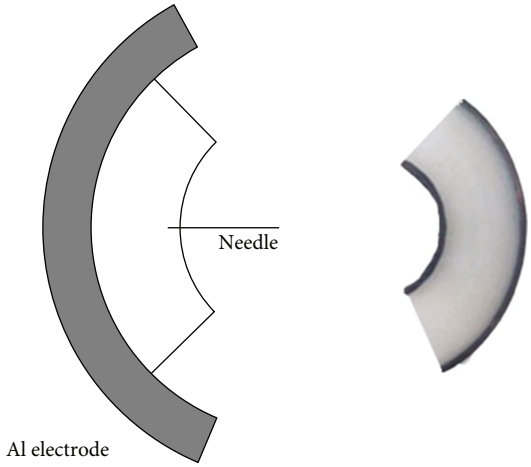

Figure 1: Sketch of the 35 kV XLPE cable slice and the needle-plate electrode.

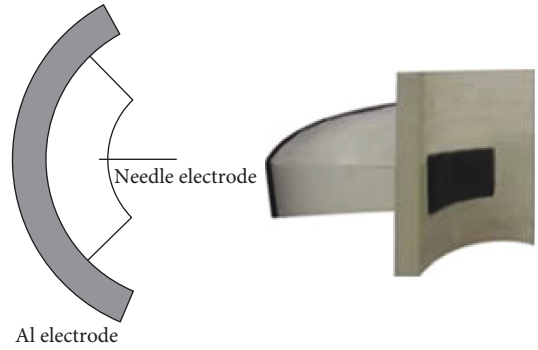

Figure 2: Sketch of the 110 kV XLPE cable slice and the needle-plate electrode.

growth of electrical trees at applied voltages. However, by combining the growth of electrical trees and the characteristics of PD in actual cable insulation, this paper studied the identification of defects in the insulation in order to provide an early warning of the breakdown of the cable insulation for the first time.

2. Experimental

2.1. Materials. Two kinds of test samples of the cable slices were used in the real-time monitoring system. One is 5 mm in thickness which was cut from 35 kV XLPE cable, and the other is 5 mm thick and were cut from 110 kV XLPE cable.

For the test samples of 35 kV cables shown in Figure 1, two semiconductive layers and XLPE insulation were kept on both sides. In order to collect clear images of the electrical trees, the surface of the translucent slices was sanded with sandpaper until it becomes glossy and smooth [20].

The electrode structure that was used to induce electrical trees was the typical needle-plate electrode. The ground electrode was made of aluminum and was close to the outer semiconductive layer. An austenitic stainless steel needle was used as the needle electrode on the high-voltage side [21, 22]. In order to narrow the difference between the induced electrical trees and the actual defects, the curvature radius of the needle tip should be as small as possible and was about $7 \pm 1\,\mu$m. After being heated, the needle tip was inserted slowly from the inner semiconductive layer 1 mm into the insulation. Heating the needle tip prevented the formation of small air gaps in the insulation when the needle was removed. The thickness of the 35 kV XLPE cable insulation was 11 mm and was 1 mm for the semiconductive shield. The distance from the needle tip to the outer semiconductive shield was about 10 mm.

The test samples of 110 kV cables were shaped as in Figure 2 in order to avoid surface flashover between the needle tip and the aluminum electrode at the rated voltage of 110 kV [23, 24]. The XLPE barriers were 7 mm in height and 1 mm thick, and both sides were processed in the cable insulation to prevent the surface slip flash discharge along the surface of the cable slices between the needle electrode and the ground electrode. The inner semiconductive layer, 5 mm wide and 1 mm thick, was reserved as shown. The thicknesses of the 110 kV XLPE cable insulation and the inner and outer semiconductive shields were 18 mm, 1.5 mm, and 1 mm, respectively. After being heated, the needle tip was inserted slowly from the inner semiconductive layer 2 mm into the insulation. The distance between the needle tips and the outer semiconductive shield was 16 mm.

2.2. Real-Time Monitoring System. The experimental system was made up of three parts. The first part was the equipment collecting the electrical tree images, which included the digital microscope, industrial control computer, and a cold light source. These images observed and collected using this part were updated four times per second in order to reflect the morphological growth of electrical trees in real time.

The second part was the PD detection system that included the testing transformer, detection sensor, oscilloscope, and industrial control computer. The detection impedance was connected to the ground loops of the samples of cable slices. The partial discharge signals detected by the impedance were magnified by the amplifier that had a magnification of 35 dB and a bandwidth of 3-40 MHz [25]. The VHF bandwidth is usually adopted in actual online monitoring.

The final part of the experimental setup was the sample of cable slices that were immersed in transformer oil and loaded in a transparent plexiglass tank. This prevents the creeping discharge and surface flashover between the needle ground electrodes. In order to collect clear and bright images of the electrical trees, the light emitted from the cold light must pass through the transparent plexiglass tank, the slice, and the transformer oil at the same time. The schematic illustration of the test system was shown in Figure 3.

2.3. Statistical PD Characteristics. The raw PD data in the growth processes of the electrical trees were sampled every two hours, and each sampling period collected 150 power frequency periods. The statistical characteristics of PD were chosen to characterize the deterioration process of the electrical trees in the XLPE cables [26, 27]. These characteristics are as follows:

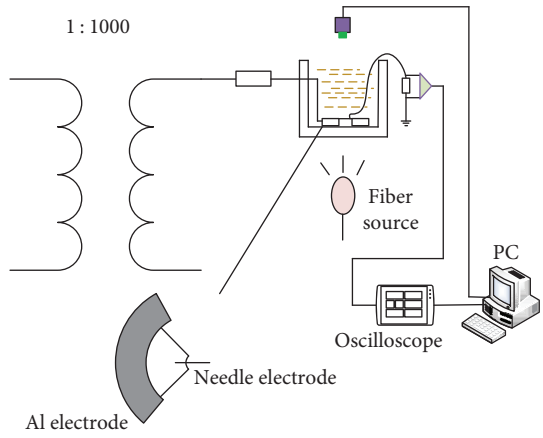

Figure 3: Schematic illustration of the test system.

q_m, the maximum discharge magnitude of PD signals in each sampling period;

q, the average discharge magnitude of PD signals in each sampling period;

U, the average discharge amplitude of PD signals in each power frequency period in each sampling period; and n, the average numbers of discharge of PD signals in each power frequency period in each sampling period.

2.4. Waveform Characteristics of PD. The equivalent time-frequency classification algorithm of the PD pulse was chosen to identify the deterioration degree. Different time-frequency features of PD waveforms at different deterioration stages provided a foundation for the identification of the deterioration degree of electrical trees [28, 29].

Considering the application in online monitoring, the feature extraction of pulse waveform should have the following characteristics: (1) real-time and fast calculations, (2) unrelated to the time record points, and (3) unrelated to the pulse amplitude and polarity. Accordingly, the data processing of a single-pulse waveform obtained from broadband detection was as follows:

$$\begin{aligned} p_j(t_i) &= \begin{cases} m_0, m_1, \cdots, m_i \cdots, m_{n-1}, \\ 0, \Delta t, \cdots \Delta t_{(i-1)} \cdots \Delta t_{(n-1)}, \end{cases} \\ P_j(f_i) &= \begin{cases} M_0, M_1, \cdots M_i, \cdots, M_{(n/2)-1}, \\ 0, \Delta f, \cdots \Delta f_{(i-1)}, \cdots, \Delta f_{((n/2)-1)}, \end{cases} \end{aligned} \tag{1}$$

where p_j is the j-th pulse; P_j is the pulse p_j's fast Fourier transform (FFT); n represents that the pulse waveform is composed of n points, and the FFT spectrum of the pulse waveform is composed of $n/2$ points; m_i is the amplitude of corresponding time domain waveform of i-th point; $\Delta t_{(i-1)}$ is the corresponding time points for the i-th point ($\Delta t = 1/f$, s is the sampling interval, f is the sampling rate, and $s = n\Delta f$); and $\Delta f_{(i-1)}$ is the frequency value of the i-th point.

In this paper, the time dispersing T and frequency dispersing F were selected to obtain the feature extraction of the pulse waveform. The processing of the pulse $p_j(t_i)$ was as follows:

$$\begin{aligned} {T_0}^j &= \frac{\sum_{i=0}^{n} t_i p_j(t_i)^2}{\sum_{i=0}^{n} p_j(t_i)^2}, \\ {F_0}^j &= \frac{\sum_{i=0}^{n/2} f_i P_j(f_i)^2}{\sum_{i=0}^{n/2} P_j(f_i)^2}, \\ (T_j)^2 &= \frac{\sum_{i=0}^{n} \left(t_i - T_0^j\right)^2 \cdot p_j^2(t_i)}{\sum_{i=0}^{n} p_j^2(t_i)}, \\ (F_j)^2 &= \frac{\sum_{i=0}^{n} \left(f_i - {F_0}^j\right)^2 \cdot {P_j}^2(f_i)}{\sum_{i=0}^{n} {P_j}^2(f_i)}. \end{aligned} \tag{2}$$

In equation (2), the mean time of the pulse waveform signal T_0^j and mean frequency F_0^j were calculated. The strike time T_j and frequency spread F_j of the pulse waveform signal were, respectively, defined as equivalent time width and equivalent bandwidth.

The 150 pulse waveforms of the PD that were collected in each sampling period were collected at a sampling rate of 1 GHz. The sampling time for each PD pulse was 1 μs so that the true PD pulse information could be fully reflected in the data. Next, 150 points appeared on the T-F diagram after the equivalent time-frequency transformed, and each point represented the equivalent time and frequency of a PD pulse waveform. On the basis of the principle of fuzzy cluster analysis, T-F points of similar waveforms could achieve good clustering performance, so the deterioration stages can be characterized using the T-F diagram.

3. Results and Discussion

3.1. Growth Characteristics of Electrical Trees of 35 kV Cables. The rated phase voltage of the 20.2 kV was evenly applied on the needle electrode and inserted into the insulation slice. The growth of electrical trees lasted about 49 hours from the starting of the electric branches to the breakdown of the entire insulation. The degradation process of the electrical trees was divided into five stages in chronological order: the early stage from 0 to the 10th hour, the early-middle stage from the 10th to 20th hour, the middle stage from the 20th to 30th hour, the middle-late stage from the 30th to 40th hour, and the late stage from the 40th to 49th hour.

The growth process of the electrical trees can be outlined as follows: the initial electrical trees expanded quickly at the early stage; stagnation-type electrical trees existed at early-middle stage; branches of electrical trees expanded quickly and developed into dendritic forms during the middle stage; the branched trees continued to expand throughout the entire insulation during the middle-late stage; at the late stage, the entire insulation was covered with electrical trees; and finally, the electric breakdown of the slice occurred. The typical states of the electrical trees from the beginning to breakdown are shown in Figure 4.

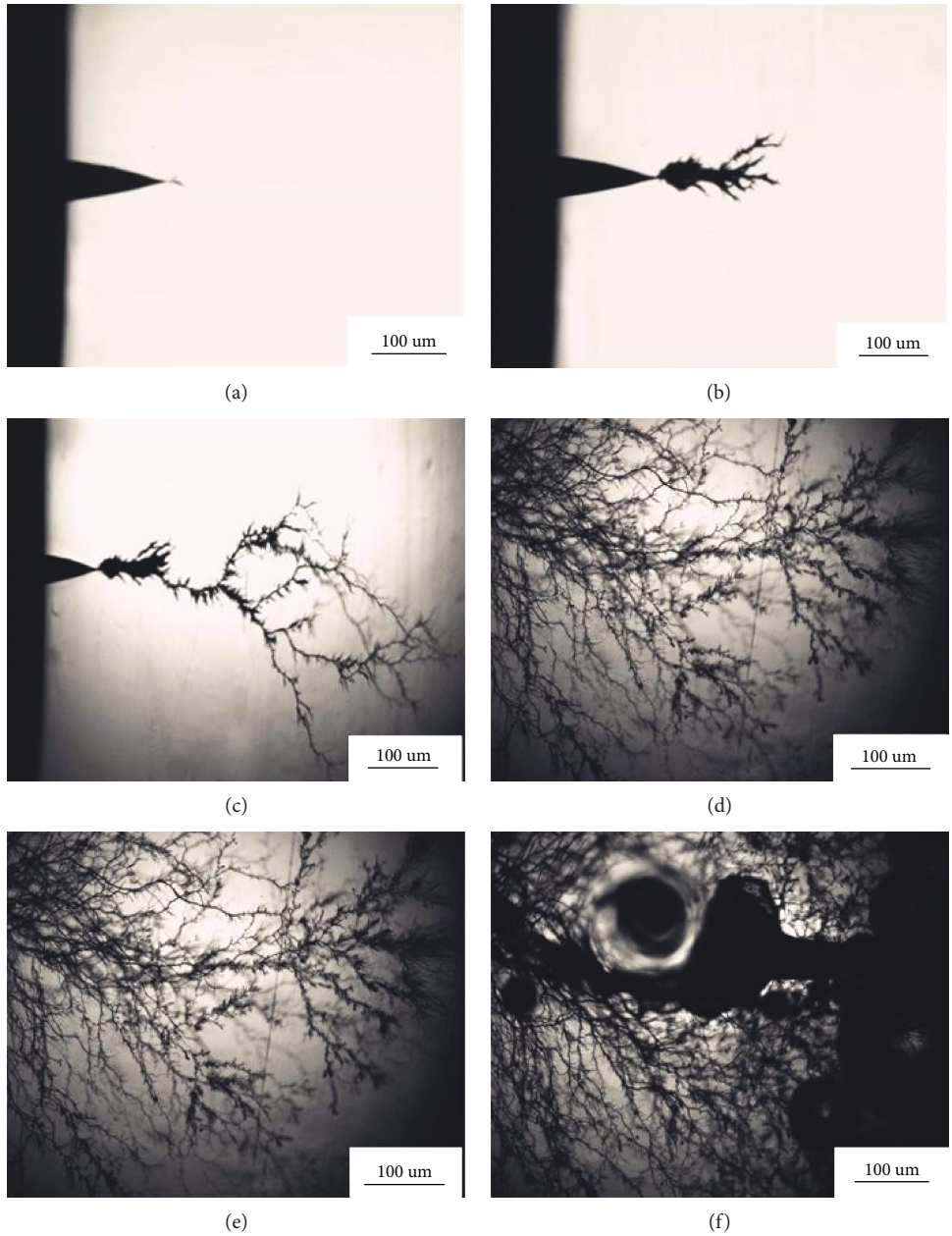

Figure 4: Deterioration process of the entire cable insulation of 35 kV cable: (a) starting, (b) 12 hours later, (c) 22 hours later, (d) 37 hours later, (e) 48 hours later, (f) breakdown.

3.2. Growth Characteristics of Electrical Trees of 110 kV Cables. The rated phase voltage of 63.5 kV was evenly applied on the needle electrode and inserted into the insulation slice. The growth of electrical trees lasted about 50 hours from the starting of the electrical trees to the breakdown of the entire insulation. The degradation process of the electrical trees was divided into five stages in chronological: the early stage from 0 to the 10th hour, the early-middle stage from the 10th to 20th hour, the middle stage from the 20th to 30th hour, the middle-late stage from the 30th to 40th hour, and the late stage from the 40th to 49th hour.

The growth process of the electrical trees in the 110 kV cable insulation was different from the 35 kV cable. The initial electrical trees grew out quickly during the early stage and expanded into a bush-like structure when high voltage was applied. The branched electrical trees grew out at the front end of the bush structure in the late period of the early stage. At the early-middle stage, the growth of electrical trees did not stagnate, but the bush-like electrical trees continued to expand. The branched electrical trees at the front end of the bush structure gradually grew and became thicker, and more subtle electrical trees appeared around the branched electrical trees. During the middle stage, some branched electrical trees developed quickly and covered the insulation in fan shapes. At the middle-late stage, the branched electrical trees continued to expand and became thicker. During the late stage, the electrical trees covered the entire insulation and reached the outer semiconductive layer and the main

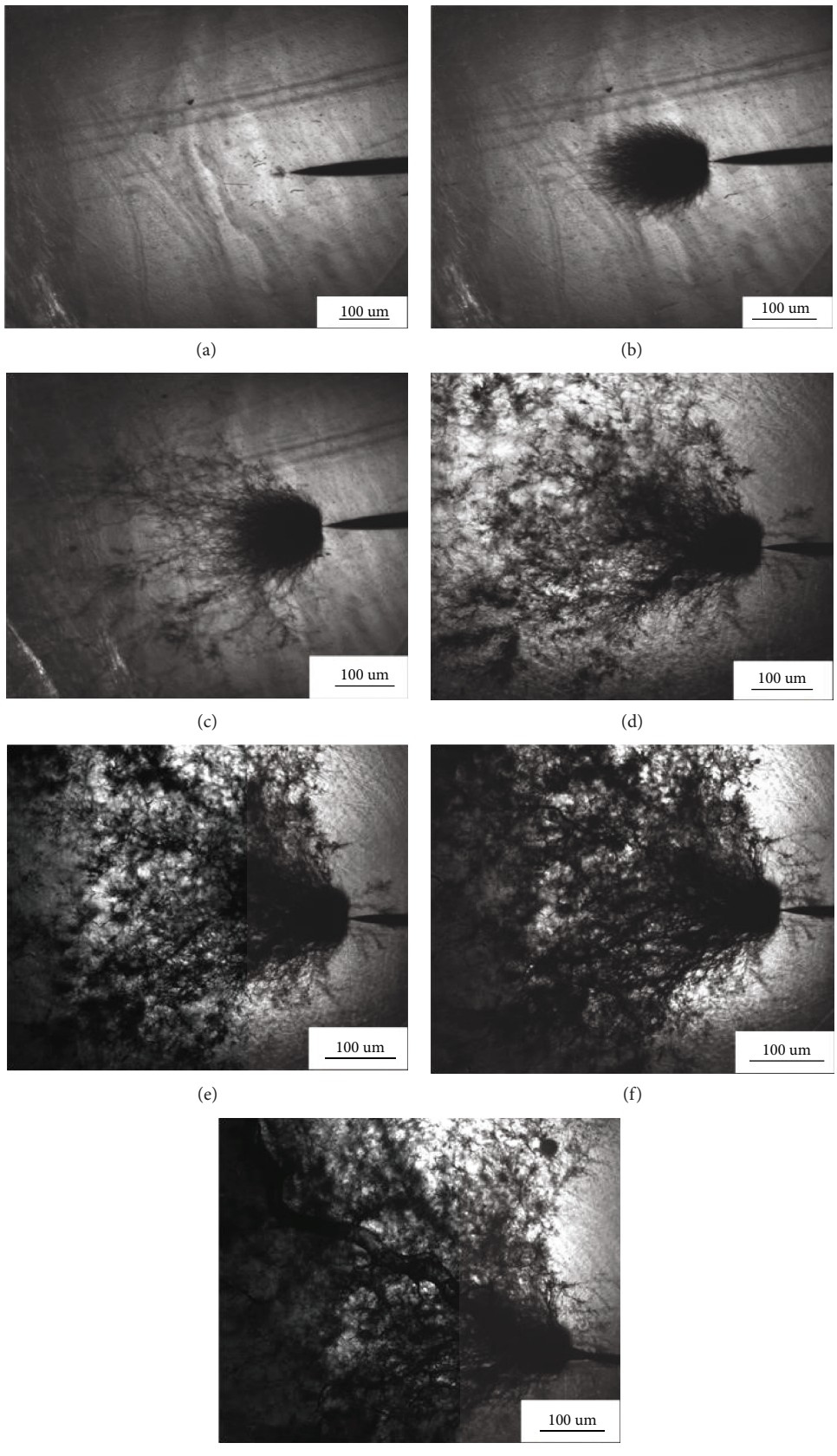

Figure 5: Deterioration process of the entire cable insulation of 110 kV cable: (a) starting, (b) 5 hours later, (c) 11 hours later, (d) 26 hours later, (e) 39 hours later, (f) 47 hours later, (g) breakdown.

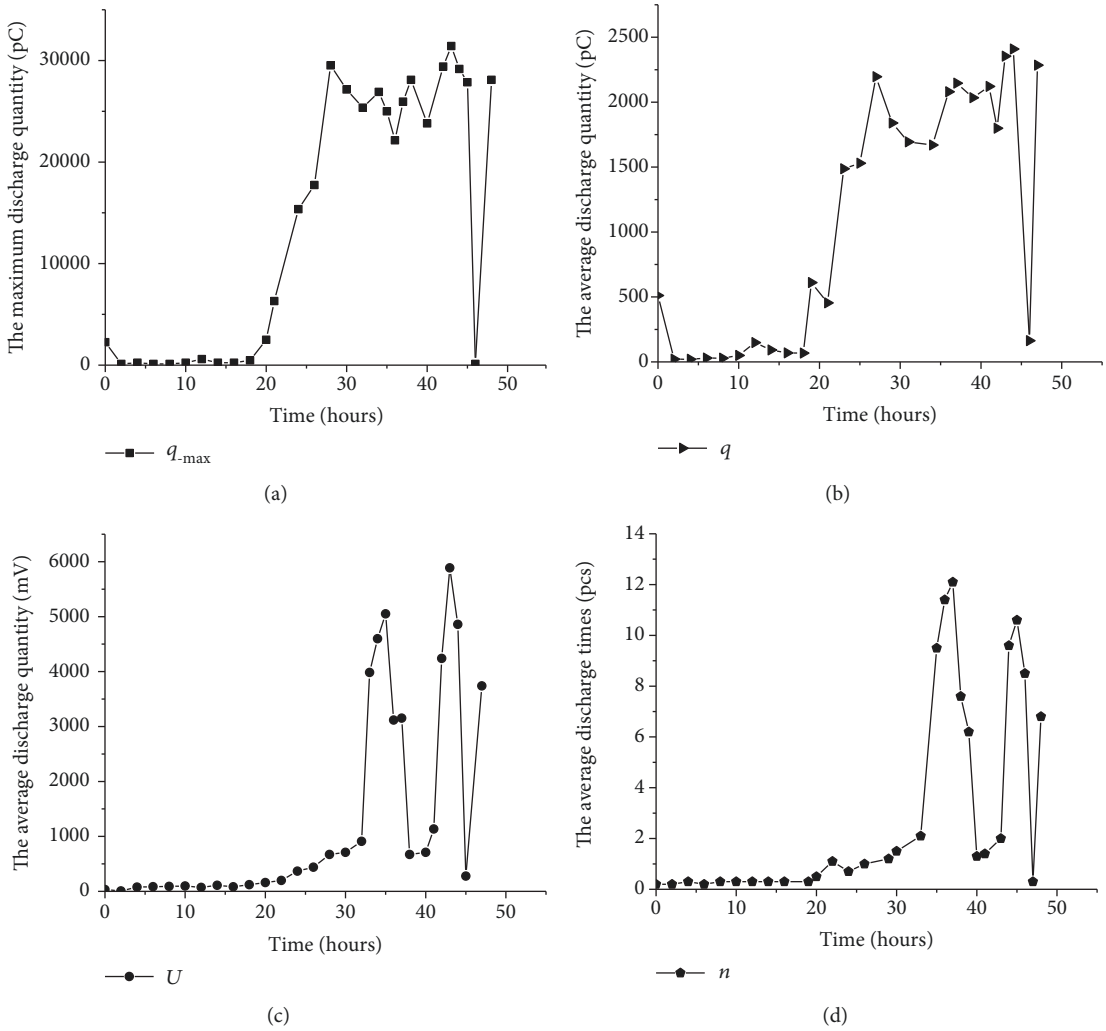

Figure 6: The changing trends of the statistical characteristics of PD in the growth process of electrical trees in 35 kV cable deterioration process of the whole cable insulation of 35 kV cable.

branches became thicker. At last, one of the main branching trees became a conductive channel and the insulation slice broke down. The typical states of the electrical trees from the beginning to breakdown are shown in Figure 5.

3.3. Statistical Characteristics of PD of 35 kV Cables. The trend graphs of q_m, q, U, and n during the entire degradation process of the electrical trees are shown in Figure 6. The q_m and q of the initial electrical trees at the early stage were larger than those of the stagnation-type electrical trees during the early-middle stage. The PD for the stagnation-type electrical trees was small and could hardly be detected. The q_m and q quickly rose during the middle stage and maintained a high and stable level before the breakdown which was far greater than at the early stage. However, U and n decreased dramatically near the 40th hour when the electrical trees reached the outer semiconductive layer. The PD had the special characteristics during this stage, with small and weak discharges, interspersed with the occasional large discharges. Additionally, the PD suddenly disappeared shortly before the breakdown and then increased rapidly for a short period before the breakdown.

3.4. Equivalent Time-Frequency Characteristics of PD Pulses at Different Deterioration Stages of 35 kV Cables. The equivalent time-frequency characteristics of the PD pulses at different deterioration stages can be summarized by quick growth of the electrical trees when the voltage was applied (Figure 7).

In the equivalent time-frequency diagram, discharges occurred in areas one and two and most were concentrated in area one, whose equivalent time width and equivalent bandwidth were from 120 to 260 ns and from 3 to 20 MHz, respectively. There were rare discharges in area two, whose equivalent time width and equivalent bandwidth were from 180 to 220 ns and from 27 to 40 MHz, respectively. Twelve hours later, the stagnation-type electrical trees occurred at the early-middle stage and all discharges were concentrated in area one, whose equivalent time width and bandwidth were from 100 to 200 ns and from 3 to 20 MHz, respectively.

Twenty-two hours later, branches of electrical trees expanded quickly and developed into a dendritic form. In the equivalent time-frequency diagram, there were discharges in both areas one and two and most of the discharges were concentrated in area two. The equivalent time widths and equivalent bandwidths of areas one and two were from

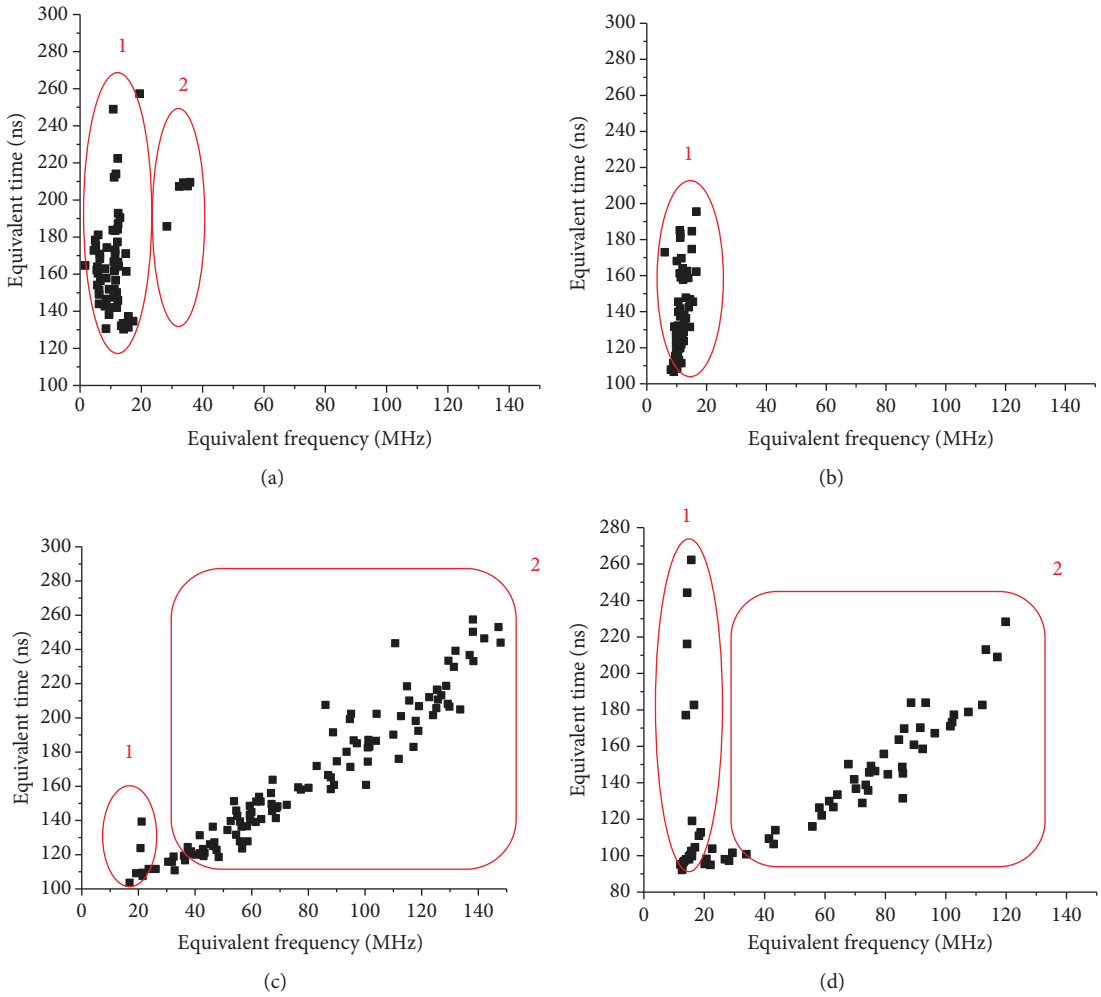

Figure 7: *T-F* clustering diagrams of PD pulse in the growth process of electrical trees in 35 kV cable: (a) starting, (b) 12 hours later, (c) 22 hours later, (d) 48 hours later.

100 to 140 ns and from 15 to 25 MHz and from 100 to 260 ns and from 25 to 150 MHz, respectively. Forty-eight hours later, the entire insulation was covered by electrical trees and almost all electrical tree clusters reached the outer semiconductive layer. At this point, the slice was about to breakdown. In the equivalent time-frequency diagram, there were discharges in both areas one and two and there were more discharges in area one than in area two. The equivalent time width and equivalent bandwidth of area one were from 90 to 260 ns and from 10 to 25 MHz, while those of area two were from 100 to 240 ns and from 25 to 125 MHz, respectively.

3.5. Statistical Characteristics of PD of 110 kV Cables. The trend graphs for the q_m, q, U, and n during the entire degradation process of the electrical trees are shown in Figure 8. The q_m and q of the initial electrical trees at the early stage were relatively large, but the discharges were small, and occasionally there were several large discharges during the early stage. The PD could not maintain a stable state during the early-middle and middle stages. Occasionally, the PD signals were small and could hardly be detected, but they were large at other times. Then, the PD maintained a stable state during the middle-late stage. Four statistical characteristics maintained a high and stable level. The PD was weakened when the electrical trees reached the outer semiconductive layer during the late stage, but increased rapidly right before the breakdown.

3.6. Equivalent Time-Frequency Characteristics of PD Pulses at Different Deterioration Stages of 110 kV Cables. The equivalent time-frequency characteristics of PD pulses at different deterioration stages are summarized as in Figure 9.

The initial electrical trees branched out quickly and expanded into a bush-like structure at the early stage. There were discharges both in areas one and two, and there were more discharges in area one than in area two. The equivalent time width and equivalent bandwidth of area one were from 430 to 540 ns and from 5 to 25 MHz, while those of area two were from 440 to 480 ns and from 25 to 40 MHz, respectively. Eleven hours later, the equivalent time width and equivalent bandwidth of area one were from 430 to 500 ns and from 10 to 25 MHz, while those of area two were from 430 to 520 ns and from 30 to 60 MHz, respectively. Twenty-six hours later, the electrical trees grew quickly. There were no discharges in

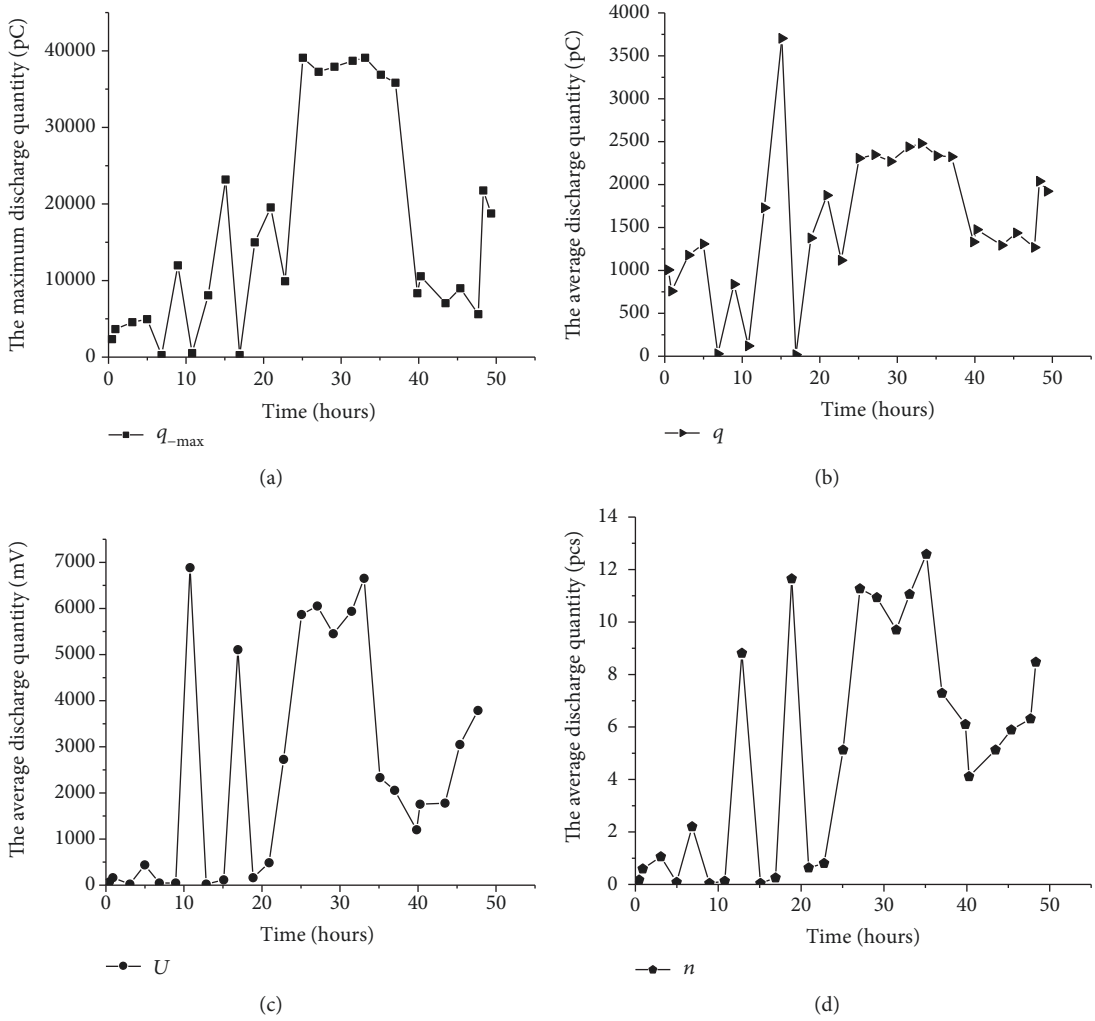

Figure 8: The changing trends of the statistical characteristics of PD in the growth process of electrical trees in 110 kV cable deterioration process of the whole cable insulation of 110 kV cable.

area one, but discharges were concentrated in area two, whose equivalent time width was from 400 to 560 ns and the equivalent bandwidth from 30 to 110 MHz as a result of the drastic growth of electrical trees. Forty-seven hours later, there were discharges in both areas one and two, but more discharges are concentrated in area two. The equivalent time width and equivalent bandwidth in area one were from 440 to 480 ns and from 10 to 35 MHz, while those in area two were from 450 to 560 ns and from 35 to 100 MHz, respectively.

4. Conclusion

In this paper, a real-time system using PDs was built to monitor the growth of electrical trees in the slices of 35 kV and 110 kV XLPE. The morphological development of the electrical trees and the characteristics of PD were studied at rated voltages. The following conclusions were drawn.

(1) The morphological development was different between the electrical trees in the 35 kV and the 110 kV XLPE. The morphology of the electrical trees in the 35 kV cable insulation was dendritic, while that in the 110 kV cable insulation contained both the bushes and the dendrites. Unlike the 35 kV, the growth of the electrical trees in the 110 kV cable insulation did not stagnate during the early-middle stage and the electrical trees reached the outer semiconductive layer well before the insulation was broken down in nearly 39 hours

(2) There were three significant statistical characteristics of the PDs during the growth of electrical trees. The first feature was that the PDs were small and could hardly be detected during the early-middle stages, although they were large when the initial electrical trees grew out. Another feature was that after growing, the PDs maintained a high and stable level during the middle and middle-late stages. The third feature was that the PDs were weakened when the electrical trees reached the outer semiconductive layer and then increased rapidly until the breakdown

(3) As shown in the equivalent time-frequency characteristics of the PD pulses, there were some similarities in the equivalent time-frequency diagram at every

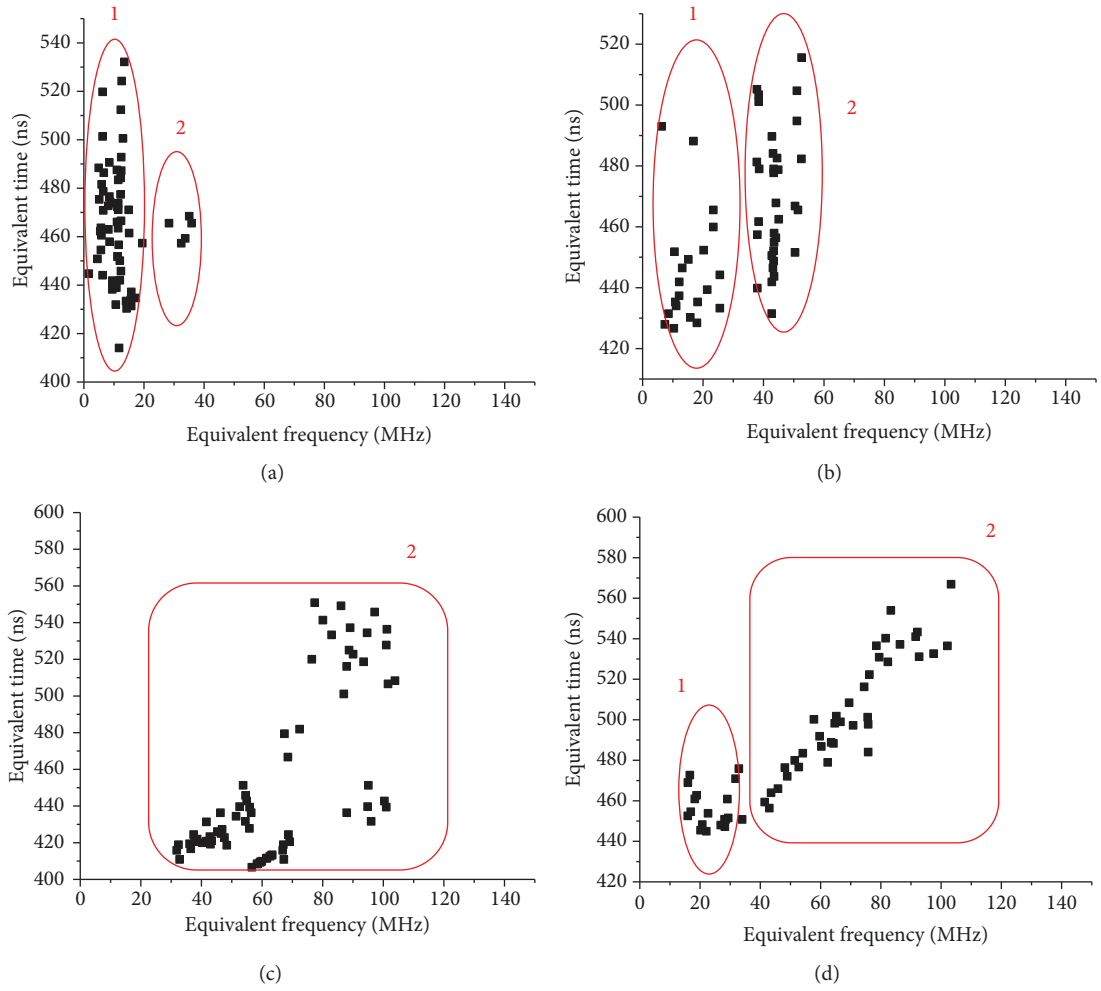

Figure 9: *T-F* clustering diagrams of PD pulse in the growth process of electrical trees in 110 kV cable: (a) starting, (b) 11 hours later, (c) 26 hours later, (d) 47 hours later.

stage in the insulation of the 35 kV and 110 kV cables. Evident characteristics such as large spans of time and frequency were present as the electrical trees grew violently in the equivalent time-frequency diagram at every stage. Such characteristics, if combined with the statistical characteristics of the PDs, could provide criteria for the identification of defects in cable insulation in order to provide an early warning of insulation breakdown in the cable

Data Availability

All authors can share the data that support the findings of the article by depositing them in a publicly available data repository wherever possible.

Conflicts of Interest

The authors declare that they have no conflicts of interest.

Acknowledgments

This research was funded by the National Basic Research Program of China (973 Program) (Grant 2009CB724506).

References

[1] X. Chen, Y. Xu, X. Cao, and S. M. Gubanski, "On the conducting and non-conducting electrical trees in XLPE cable insulation specimens," *IEEE Transactions on Dielectrics and Electrical Insulation*, vol. 23, no. 1, pp. 95–103, 2016.

[2] H. Sui, L. M. Shen, W. Wang, Y. L. Yu, Z. Wang, and C. F. Gao, "PD detecting during the growth of electrical trees in HV XLPE cable," in *2011 Asia-Pacific Power and Energy Engineering Conference*, pp. 1–4, Wuhan, China, March 2011.

[3] Y. Wang, K. Xiao, C. Wang, L. Yang, and F. Wang, "Effect of nanoparticle surface modification and filling concentration on space charge characteristics in TiO_2/XLPE nanocomposites," *Journal of Nanomaterials*, vol. 2016, Article ID 2840410, 10 pages, 2016.

[4] B. Quak, E. Gulski, F. J. Wester, and P. N. Seitz, "Advanced PD site location in distribution power cables," in *Proceedings of the*

7th International Conference on Properties and Applications of Dielectric Materials (Cat. No.03CH37417), pp. 183–186, Nagoya, Japan, 2003.

[5] J. Kuffel and P. Kuffel, *High Voltage Engineering Fundamentals*, Elsevier, 2000.

[6] N. Rouha and A. Beroual, "Modelling the treeing growth, currents and loss factor in solid electrical insulations with and without tree," in *International Conference on Electrical Engineering, Electronics and Automatics ICREA*, pp. 135–138, Bejaïa, Algeria, 2010.

[7] C. Wang, Y. Wang, P. Fan, and R. Liao, "Space charge property of polyethylene/silica nanocomposites at different elongations," *Journal of Nanomaterials*, vol. 2015, Article ID 963960, 14 pages, 2015.

[8] X. L. Zhang, Z. H. Wang, Z. Y. Huang, and X. J. Han, "The design of high-voltage cable partial discharge on-line monitoring system software," *Applied Mechanics and Materials*, vol. 672-674, pp. 810–813, 2014.

[9] Y. Wang, Y. Wang, C. Wang, and H. Xu, "The partial discharge characteristic of typical XLPE cable insulation defects under damped oscillating voltage," in *2014 IEEE Electrical Insulation Conference (EIC)*, pp. 290–293, Philadelphia, PA, USA, 2014.

[10] A. H. A. Bakar, H. Mokhlis, H. A. Illias, and P. L. Chong, "The study of directional overcurrent relay and directional earth-fault protection application for 33 kV underground cable system in Malaysia," *International Journal of Electrical Power & Energy Systems*, vol. 40, no. 1, pp. 113–119, 2012.

[11] W. Zheng, Y. Qian, N. Yang, C. Huang, and X. Jiang, "Research on partial discharge localization in XLPE cable accessories using multi-sensor joint detection technology," *Przegląd Elektrotechniczny*, vol. 87, no. 11, pp. 84–88, 2011.

[12] J. G. Gao, H. Zhang, L. L. Li, J. Zhang, N. Guo, and X. H. Zhang, "Study on space charge of XLPE/O-MMT Nanocomposites," *Acta Polymerica Sinica*, vol. 13, pp. 126–133, 2013.

[13] X. Chen, Y. Xu, X. Cao, S. Dodd, and L. Dissado, "Effect of tree channel conductivity on electrical tree shape and breakdown in XLPE cable insulation samples," *IEEE Transactions on Dielectrics and Electrical Insulation*, vol. 18, no. 3, pp. 847–860, 2011.

[14] H. Wang, J. He, X. Zhang, Z. Li, L. Li, and G. Guan, "Electrical tree inception characteristics of XLPE insulation under power-frequency voltage and superimposed impulse voltage," in *11th International Symposium on High-Voltage Engineering (ISH 99)*, pp. 320–323, London, UK, 1999.

[15] M. Bao, X. Yin, and J. He, "Structure characteristics of electrical treeing in XLPE insulation under high frequencies," *Physica B: Condensed Matter*, vol. 406, no. 14, pp. 2885–2890, 2011.

[16] J. Yang, C. Liu, C. Zheng, H. Zhao, X. Wang, and M. Gao, "Effects of interfacial charge on the DC dielectric properties of nanocomposites," *Journal of Nanomaterials*, vol. 2016, Article ID 2935202, 11 pages, 2016.

[17] A. El-Zein, M. Talaat, and M. El Bahy, "A numerical model of electrical tree growth in solid insulation," *IEEE Transactions on Dielectrics and Electrical Insulation*, vol. 16, no. 6, pp. 1724–1734, 2009.

[18] Z. Jing, C. Li, H. Zhao, G. Zhang, and B. Han, "Doping effect of graphene nanoplatelets on electrical insulation properties of polyethylene: from macroscopic to molecular scale," *Materials*, vol. 9, no. 8, p. 680, 2016.

[19] F. Komori, D. Asai, Y. Suzuoki, and T. Kawahara, "Electrical tree in the crosslinked polyethylene with bowtie trees and the partial discharge occurrence phase angle distribution," in *Proceedings of 2014 International Symposium on Electrical Insulating Materials*, pp. 176–179, Niigata City, Japan, 2014.

[20] L. M. Yang, Z. E. Zhu, R. K. Yang, Y. Yang, and Y. Wang, "Insulation material and structure design of HVDC flexible cables," *Automation of Electric Power Systems*, vol. 37, pp. 117–124, 2013.

[21] M. Eesaee, E. David, N. R. Demarquette, and D. Fabiani, "Electrical breakdown properties of clay-based LDPE blends and nanocomposites," *Journal of Nanomaterials*, vol. 2018, Article ID 7921725, 17 pages, 2018.

[22] C. Laurent, F. Massines, and C. Mayoux, "Optical emission due to space charge effects in electrically stressed polymers," *IEEE Transactions on Dielectrics and Electrical Insulation*, vol. 4, no. 5, pp. 585–603, 1997.

[23] Suwarno, Y. Suzuoki, F. Komori, and T. Mizutani, "Partial discharges due to electrical treeing in polymers: phase-resolved and time-sequence observation and analysis," *Journal of Physics D: Applied Physics*, vol. 29, no. 11, pp. 2922–2931, 1996.

[24] W. Chang, C. Li, Q. Su, and Z. Ge, "Study on development of partial discharges at the defect caused by a needle damage to a cable joint," *Zhongguo Dianji Gongcheng Xuebao*, vol. 33, no. 7, pp. 192–201, 2013.

[25] Suwarno, "Partial discharge in high voltage insulating materials," *International Journal on Electrical Engineering and Informatics*, vol. 8, no. 1, pp. 147–163, 2016.

[26] T. Kumazawa, "Application of the AC superposition method to degradation diagnosis of 22/33-kV class XLPE cables," *Electrical Engineering in Japan*, vol. 195, no. 1, pp. 32–39, 2016.

[27] B. Jonuz, P. H. F. Morshuis, H. J. Van Breen, J. Pellis, and J. J. Smit, "Detection of water trees in medium voltage XLPE cables by return voltage measurements," in *2000 Annual Report Conference on Electrical Insulation and Dielectric Phenomena (Cat. No.00CH37132)*, pp. 355–358, Victoria, BC, Canada, 2000.

[28] J. Lin, J. Gui, S. Gao et al., "Propagation characteristics of partial discharge pulses in the cable," *Journal of Power and Energy Engineering*, vol. 2, no. 9, pp. 112–116, 2014.

[29] E. Ouatah, S. Megherfi, K. Haroun, and Y. Zebboudj, "Characteristics of partial discharge pulses propagation in shielded power cable," *Electric Power Systems Research*, vol. 99, pp. 38–44, 2013.